RSC Advances

PAPER

Cite this: *RSC Adv.*, 2023, **13**, 30885

Adsorption and decolorization study of reactive black 5 by immobilized metal–organic framework of UiO-66 and *Gloeophyllum trabeum* fungus

Taufiq Rinda Alkas, [a] Adi Setyo Purnomo, *[b] Ratna Ediati[b] and Taslim Ersam[b]

Received 7th June 2023
Accepted 14th October 2023

DOI: 10.1039/d3ra03804a

rsc.li/rsc-advances

This study aimed to investigate immobilized metal–organic framework (MOF) UiO-66 and brown-rot fungus *Gloeophyllum trabeum* (GT) in PVA-SA matrices for adsorption and decolorization of reactive black 5 (RB5). Furthermore, UiO-66/GT@PVA-SA composite was successfully fabricated and obtained by immobilizing UiO-66 and GT mycelia into a mixture of PVA-SA. This composite demonstrated a decolorization ability of 80.12% for RB5 after 7 days. The composite's reusability was assessed for three cycles; at last, it only achieved 21%. This study reported that adsorption of RB5 by the composite followed a pseudo-second-order kinetic model with a correlation coefficient (R^2) of 0.9997. The Freundlich model was found to be suitable for the isotherm adsorption. The process was also spontaneous and feasible, as indicated by the negative ΔG value. Subsequently, four metabolite products resulting from decolorization of RB5 by UiO-66/GT@PVA-SA composite were proposed, namely: $C_{24}H_{19}N_5Na_2O_{13}S_4$ (m/z = 762), $C_{10}H_{13}N_2O_8S_2^-$ (m/z = 353), $C_{12}H_9N_4O_7S_2^-$ (m/z = 384), and $C_{10}H_{13}O_8S_2^-$ (m/z = 325).

1 Introduction

Water bodies worldwide are facing pollution issues due to synthetic dye waste from various industries that uses dyes. The textile industry is the largest consumer of dyestuffs compared to other sectors. This industry is considered to be the oldest field of the global economy and remains the world's largest industry. It employs a large number of workers worldwide (1.5 million in Brazil and 8 million in China) and produces a large amount of textiles (1.3 million tons in Brazil and 79.29 million tons in China).[1–4] Unfortunately, these waste products can lead to health problems such as kidney, reproductive system, liver, brain, and central nervous system dysfunction,[5] and pose a threat to the environment and organisms due to their high toxicity and persistent compounds.[6]

To address the issue of synthetic dye waste causing pollution in water bodies, various methods have been developed, including physical and chemical treatments. However, these methods have technical or economic drawbacks, making them unaffordable for the low-income textile printing and dyeing industry.[7] Alternative method that is considered efficient for treating dye waste is the biodegradation method, which uses bacteria and fungi to treat the waste because it is affordable and more environmentally friendly.[8,9] Brown-rot fungus *Gloeophyllum trabeum* (GT) was used in the biodegradation process of some synthetic dyes because of its enzymes and a Fenton reaction mechanism. The Fenton reaction is one of the least expensive methods for Advanced Oxidation Processes (AOPs) that use ferric ions to catalyze the formation of hydroxyl radicals and the subsequent mineralization of organic to CO_2, H_2O, and lower organic acids.[10] Some dyes that have been studied for degradation by this fungus include Methyl Orange, Methylene Blue, Methyl Green, Remazol Brilliant Blue R, Remazol Brilliant Yellow GL, Remazol Brilliant Orange 3R, Reactive Blue 4, Remazol Brilliant Red F3B, and Reactive Black 5.[11–15]

However, the pollutant biodegradation process using free cells still has some drawbacks, such as the cells used are limited in terms of operational stability, reusability, and transfer of substrates into cells.[16] Cell immobilization is a solution that overcomes this drawback. According to Couto, fungal immobilization has advantages over using free fungal cells, such as its reusability, easier solid–liquid separation, minimal clogging in continuous flow systems.[17] Immobilization is a technology that has been developed to safeguard the core material or microbial cells against environmental toxicity during adsorption or degradation of chemicals or pollutants. This study utilizes PVA and SA matrices as immobilization materials to prevent cell damage. According to Liu *et al.*, combining the natural matrix with the synthetic matrix can overcome these weaknesses and even provide complementary advantages with the right combination.[18] Furthermore, Hu *et al.* reported that tannic acid-PVA/SA hydrogel beads have effective properties for methylene blue

[a]*Departement of Environment Management, Politeknik Pertanian Negeri Samarinda, Samarinda, 75131, Indonesia*

[b]*Department of Chemistry, Institut Teknologi Sepuluh Nopember (ITS), Surabaya, 60111, Indonesia. E-mail: adi_setyo@chem.its.ac.id*

absorption compared to other adsorbents depending on the maximum capacity.[19]

In this study, GT fungus was combined with a pore material, namely metal–organic framework (MOF). This material generated a large number of investigations in the fields of catalysis, adsorption and separation, gas storage, and drug delivery.[20] Fungus cells were immobilized with MOF into supporting materials such as Polyvinyl Alcohol (PVA) and Sodium Alginate (SA). One type of MOF that has a biocompatible property with fungus is Universitetet i Oslo-66 (UiO-66), which has advantages such as high thermal stability (up to 540 °C), large surface area, high porosity, and resilience in aqueous media.[21] Subsequently, this study continues a previous study using a different dye (RB5) on the same material. A previous study found that the beads could remove 88.29% of the methylene blue (MB) dye after 72 h. This study investigated RB5 dye degradation, including the kinetic, isotherm, and thermodynamic adsorption aspects and the influence of dye concentration, pH, and temperature parameters. Optimum conditions for the RB5 dye degradation process were tested using the Box-Behnken experimental design and Response Surface Methodology (RSM). The metabolite products from the degradation were identified, and the degradation pathway was proposed.

2 Experimental section

2.1 Materials

The stock culture of *G. trabeum* NBRC 6509 fungus was purchased from the NITE Biological Resource Center (NBRC, Chiba). The chemicals used include demineralized water (DM; Brataco), ethanol (70%; SAP Chemicals), zirconium(IV) tetrachloride ($ZrCl_4$, 99%, Sigma-Aldrich), benzene-1,4-dicarboxylic acid (H_2BDC, 97%, Sigma-Aldrich), *N*,*N*-dimethyl-formamide (DMF, 99%, Sigma-Aldrich), glacial acetic acid (CH_3COOH, 100%, Merck), chloroform (CH_3Cl, 99.99%, Merck), methanol (CH_3OH, 99%, Merck), reactive black 5 (RB5; Sigma Aldrich), Polyvinyl alcohol (PVA with Mw. approx. 60 000; Merck), $CaCl_2 \cdot 2H_2O$ (≥99%, SAP Chemicals), boric acid (>99.5%, SAP Chemicals), sodium alginate (SA; HiMedia), potato dextrose broth (PDB; HiMedia), and potato dextrose agar (PDA; Merck).

2.2 Culture condition

The stock culture from a solid media (PDA) was regenerated into a new media. Fungus was inoculated into a Petri dish containing PDA media (±20 mL) which was sterilized by autoclaving at 121 °C for 20 min. Then fungus culture was incubated at 30 °C for 7 days. The solid culture was homogenized after 7 days with DM and inoculated into PDB media at 30 °C. After seven days, the mycelia were used in the following immobilization steps.

2.3 Synthesis of UiO-66

The synthesis of UiO-66 was carried out using the method from Ediati *et al.*[21] with some modifications. Initially, two precursor solutions were made by adding 1.75 g of $ZrCl_4$ and 12.5 g of H_2BDC each to two different Pyrex bottles containing 75 mL of DMF solvent, stirred with a magnetic stirrer for 15 min. Then, the precursor solution containing H_2BDC was added, 21.5 mL of glacial acetic acid was stirred again for 15 min. The two precursor solutions were then mixed and stirred again for 30 min. The mixture was heated in an oven at 120 °C for 24 h; after cooling for 24 h, the filtrate was separated by decanting. The UiO-66 precipitate obtained was added and decanted with DMF and chloroform periodically alternating 24 h and stored at room temperature. On the third day, methanol was added to the UiO-66 precipitate and left for 24 h. Finally, the precipitate was dried in an oven at 90 °C for 2 h after decanting.

2.4 Immobilization of UiO-66 and GT fungus

This process is in line with our previous study (Alkas *et al.*[22]) with some modifications, 0.1% (w/v) UiO-66 in 100 mL DM, regenerated fungus biomass 5% (w/v) from liquid culture and PVA (4% w/v). Furthermore, 1–3% (w/v) variation in SA was added to the mixture. Fungus suspension containing UiO-66 was then homogenized with a hand homogenizer for ±10 min. This mixture was then slowly added dropwise by a sterile syringe (10 mL capacity) into a cold mixture of 4% (w/v) $CaCl_2$ and 2% (w/v) boric acid that was stirred with a magnetic stirrer. The formed beads were left for ±24 h, and the beads were filtered and washed with distilled water to remove the $CaCl_2$ and boric acid mixture. Additionally, the resulting beads were stored in the refrigerator before application, and the beads were characterized using SEM-EDX, XRD, FTIR, and TGA instruments.

2.5 Characterization

UiO-66/GT@PVA-SA beads before and after decolorization were characterized using SEM-EDX (JEOL JSM 6010LV) to determine composite morphology and constituent elements. Before characterized, the beads were freeze-dried at −40 °C and vacuumed in a freeze dryer for approximately 5 h. To see the morphology of the cross-sectional surface, the sample is sliced and coated through a coating process first. SEM-EDX analysis was carried out at various magnifications and mapping of the elements contained in the beads was carried out.

The crystal structure of the material was characterized using an X-ray diffractometer (XRD-JEOL JDX-3530). The light source used is Cu Kα radiation ($\lambda = 1.5406$ Å), with a voltage of 40 kV and a current of 30 mA. Analysis was carried out at short angles with a range of 2θ from 5–50°. FTIR spectra were obtained using a Shimadzu Instrument Spectrum One 8400S at 500 to 4000 cm^{-1} wave numbers. The beads from the freeze-dryer were crushed and made into KBr pellets. The thermal stability of the UiO-66 and the UiO-66/GT@PVA-SA beads were studied with a TGA instrument (Mettler Toledo, TGA/DSC1). The synthesized sample was weighed at 10 mg and then placed in a holder to be heated at a rate of 10 °C min^{-1} at 30–600 °C with airflow.

2.6 Dye decolorization by UiO-66/GT@PVA-SA

To determine the optimum concentration of SA, decolorization test was conducted with RB5 (50 mg L^{-1}). Each of the various beads (1–3% SA) was placed in Erlenmeyer, and then 100 mL of RB5 solution was added and stored in an incubator at 30 °C.

Samples were pipetted and absorbance was measured with a UV-vis spectrophotometer on days 1, 3, 5 and 7. The best decolorization rate on the 7th day became a reference for the selection of SA concentration for further tests.

Other compositions were also used as a comparison, including GT@PVA-SA, UiO-66@PVA-SA, and UiO-66/GT(dead fungus)@PVA-SA. Decolorization results of the four kinds of beads were compared, especially on the 7th day. Subsequently, before measuring the absorbance, the solution was centrifuged at 3000 rpm for 10 min, and the supernatant was measured for its absorbance at a wavelength range of 300–800 nm. Decolorization rate was calculated at the peak wavelength exhibiting the highest absorption based on eqn (1):[23]

$$\text{Decolorization}(\%) = \frac{(A_o - A_t)}{A_o} \times 100\% \quad (1)$$

where A_o represents the absorbance of the control solution (dye) and A_t is the absorbance at time t. While, adsorption capacity at time t (Q_t, mg g^{-1}) is given by eqn (2):[24]

$$Q_t = \frac{(C_o - C_t) \times V}{W} \quad (2)$$

where C_o denotes the initial concentration (mg L^{-1}), C_t is the concentration at time t (mg L^{-1}). While V and W are the adsorbate volume (L) and the adsorbent mass (g), respectively.

The reuse test was also performed to determine the ability of the beads to be used repeatedly in decolorization process. The tests carried out were similar to decolorization test, but after the first use, the beads were then washed with DM 2–3 times and then reused (applied to a new RB5 solution) and so on for up to three cycles.

2.7 Adsorption tests

2.7.1 Determination of the mass of the beads in RB5 adsorption test. UiO-66/GT@PVA-SA beads were weighed at 1, 3, 5 and 7 g (wet weight), then each was placed in a 100 mL Erlenmeyer containing 20 mL of dye solution. Then the absorbance of the supernatant from the sample centrifugation was measured with a UV-vis spectrophotometer at the maximum wavelength of RB5. This experiment was carried out with two replications for 7 days. The determination of the number of beads used in the next adsorption test was obtained from the ratio index value between the percent decolorization and the mass of the beads. The highest index value becomes the reference for the number of beads used next.

2.7.2 Effect of contact time. From the previous experiment, the mass of the beads was determined, which allows for observing the influence of the contact time. Three grams of beads were selected to be added to 20 mL of RB5 solution (50 mg L^{-1}). The test was carried out at a time variation of 10–120 min at 30 °C and shaken with an orbital shaker (120 rpm). After adsorption, the sample was centrifuged and measured with a UV-vis spectrophotometer.

2.7.3 Adsorption kinetics. RB5 dye adsorption test was conducted by adding ±3 g beads to 20 mL of RB5 solution (50 mg L^{-1}), and the test was performed at 10–120 min at 30 °C and shaken with an orbital shaker at 120 rpm. After adsorption, the sample was centrifuged at 3000 rpm for 10 min. Next, the supernatant was measured for its absorbance with a UV-vis spectrophotometer at λ_{max} of RB5.

The data were processed using Microsoft Excel to obtain the linear regression equation and the correlation coefficient (R^2). These data were then plotted to pseudo-first-order and pseudo-second-order kinetic models. The equations model were displayed in eqn (3) and (4) as follows:[25,26]

$$\ln(q_e - q_t) = \ln q_e - k_1 t \quad (3)$$

$$\frac{t}{q_t} = \frac{1}{k_2 q_e^2} + \frac{1}{q_e} t \quad (4)$$

where q_e represents adsorption capacity at equilibrium, q_t is adsorption capacity at time t, and t is the contact time. While k_1 and k_2 are the pseudo-first-order and pseudo-second-order adsorption rate constants, respectively.

2.7.4 Isotherm adsorption. In this study, the focus was solely on the Langmuir and Freundlich model, which is commonly cited in study reports on dye adsorption. The Langmuir isotherm model is frequently employed by environmental adsorption researchers due to its compatibility with low temperatures, ease of use, and flexibility with computer simulations, especially when coupled with equations of displacement phenomena.[27] The mathematical equation for the Langmuir isotherm is as follows:[24]

$$\frac{1}{Q_e} = \frac{1}{Q_m} + \frac{1}{Q_m \times K_L \times C_e} \quad (5)$$

where C_e is the equilibrium concentration (mg L^{-1}), Q_e is the equilibrium adsorption capacity (mg g^{-1}), K_L is the isotherm constant (L mg^{-1}), and Q_m is the maximum adsorption capacity (mg g^{-1}).

The Freundlich isotherm model describes the type of adsorption of physics where adsorption occurs in several layers, and the bond is not strong. The mathematical equation of this model is based on the assumption that the adsorbent has a heterogeneous surface and each molecule has a different absorption potential.[28] This model is shown in eqn (6):[29]

$$\ln Q_e = \ln K_F + \frac{1}{n} \ln C_e \quad (6)$$

where K_F is the Freundlich isotherm constant and n: adsorption intensity, C_e and Q_e are the concentration (mg L^{-1}) and adsorption capacity (mg g^{-1}) at equilibrium, respectively.

The Langmuir and Freundlich isotherm adsorption models were employed to test UiO-66/GT@PVA-SA composite capacity for RB5 adsorption. The test was carried out by adding the beads to various concentrations of RB5 (50, 100, 150, 200, 250, and 500 mg L^{-1}). After reaching the equilibrium time obtained from testing the contact time variation, the sample solution was then centrifuged and measured the absorbance.

2.7.5 Adsorption thermodynamics. To determine the level of the spontaneity of adsorption process, study of adsorption thermodynamics was conducted. This experiment involved shaking UiO-66/GT@PVA-SA composite with RB5 solutions of

50 mg L^{-1} concentration at various temperatures (20, 30, and 40 °C) and time variations (10–120 min). The estimated thermodynamic parameters are Gibbs free energy (ΔG), entropy change (ΔS), enthalpy change (ΔH), and the equilibrium distribution constant (K_d). The equilibrium distribution constant is related to (ΔH) and (ΔS) as shown in eqn (7), where T (K) is the absolute temperature. Based on the relationship between ΔG^0 and K_d, changes in the equilibrium constant with temperature can be obtained from the following eqn (7)–(9):[30]

$$\ln K_d = \frac{\Delta S}{R} - \frac{\Delta H}{RT} \quad (7)$$

$$K_d = \frac{C_{ad,e}}{C_e} \quad (8)$$

$$\Delta G = \Delta H - T\Delta S \quad (9)$$

The values of ΔH and ΔS were determined from the slope and ordinates values of the $\ln K_d$ *vs.* $1/T$ graph. At the same time, the K_d value was obtained from a comparison of the dye concentration in the adsorbent ($C_{ad,e}$, mg L^{-1}) and the equilibrium concentration of the adsorbate (C_e) shown in eqn (8). Then the ΔG value was determined by eqn (9).[31]

The data obtained from the temperature variations above were plotted $1/T$ against $\ln K_d$ to become a scatter graph. To find the linear regression equation by using Microsoft Excel, the constant R in this equation was an ideal gas constant with a value of 8.314 Joule mol^{-1} K^{-1}. Enthalpy change (ΔH) was obtained by multiplying the gradient by R, while the intercept value multiplied by R was used to determine the entropy change (ΔS).

2.7.6 RB5 decolorization mechanism. The mechanism of RB5 decolorization process was observed with two instruments, namely HPLC and UV-vis spectrophotometer. The HPLC analysis was carried out by taking the supernatant from a 50 mg L^{-1} concentration sample of RB5 solution treated with UiO-66/GT@PVA-SA biocomposite (±3 g) for 12, 24, 36, and 48 h variation. RB5 control solution with a concentration of 50 mg L^{-1} was used to compare the chromatogram results obtained. A UV-vis spectrophotometer analysis with more time variation from 10 to 2880 min was also performed to determine the rate of decolorization and plotted to get a decolorization rate *versus* time and then for the decolorization mechanism that occurred.

2.8 Optimization using RSM

To determine the relationships between the independent variables and the response, RSM method was employed. The resulting equation model can be used to predict the optimum response for the desired outcome. In this study, the percent decolorization response was analyzed across three independent variables, namely dye concentration, pH, and incubation temperature. Decolorization rate response was represented as Y, while X_1, X_2, and X_3 represented each independent variable. The other variables such as contact time, amount of UiO-66, number of beads, amount of dye solution followed the previous procedure, and the air pressure/ambient conditions were not changed. The Box-Behnken design was used with 15 treatment variants, and the procedure was performed using the Design Expert software. The variant number of this treatment is obtained by calculating practical numbers based on the following formula (eqn (10)):[32,33]

$$N = K^2 + K + C_P \quad (10)$$

where K is the number of factors, three variables in this study, and C_p is the central point set to 3. Finally, the experimental runs are 15 from the formula. Meanwhile, the experimental results were fitted into a second-order equation (eqn. (11)):[33]

$$y = \beta_0 + \beta_1 X_1 + \beta_2 X_2 + \beta_3 X_3 + \beta_{11} {X_1}^2 + \beta_{22} {X_2}^2 + \beta_{33} {X_3}^2 + \beta_{12} X_1 X_2 + \beta_{13} X_1 X_3 + \beta_{23} X_2 X_3 \quad (11)$$

where y is the response of RB5 decolorization percentage, β_0, β_1, β_2, and β_3 are linear interaction coefficients; β_{11}, β_{22}, and β_{33} are related to the quadratic coefficients; and β_{12}, β_{13}, β_{23} are denoted as the interaction coefficents, while X_1, X_2, and X_3 designate as independent variables. Table 1 shows the assessment intervals for each of the three independent variables investigated.

Table 1 The limits of the variables used

	Scale		
Variables	−1	0	1
X_1: RB5 initial concentration (mg L^{-1})	50	100	150
X_2: pH	4	7	10
X_3: Temperature (°C)	20	30	40

2.9 Identification of metabolite products with LCMS

This analysis was performed to predict the metabolite product of RB5 dye decolorization that occurred in UiO-66/GT@PVA-SA composites for comparison using a standard RB5 solution. The identification was carried out on the supernatant resulting from centrifugation of decolorized samples after the 7th day. This analysis was performed with the LCMS-2010SA (Shimadzu, Japan) using the method developed by Usha *et al.*[34] with a C18 column (4.6 mm × 250 mm). The mobile phase was methanol/water (50 : 50 v/v), and the UV detector (254 nm) was used. The mobile phase flowed at 0.6 mL min^{-1} and 10 µl of the sample was injected. Furthermore, its MS spectra were acquired using an ion trap mass spectrometer coupled to an electrospray interface (ESI, Thermo Finnigan LCQ-DUO, USA). The apparatus was operated in negative ionization mode with a spray voltage of 4.5 kV, capillary temperature of 275 °C, sheath gas of 40 AU (arbitrary units), and auxiliary gas of 26 AU.

3 Results and discussions

3.1 Immobilization of MOF UiO-66 and GT fungus

The results of immobilizing UiO-66 and GT in PVA-SA can be seen visually in Fig. 1, where the shape of the beads obtained is

Fig. 1 Immobilization product of MOF UiO-66 and GT fungus in PVA-SA matrices.

almost perfectly round with a brownish-white color. After evaluating various concentrations of SA, 2% (w/v) was found to be the most suitable for creating immobilized beads with a desirable round shape and hardness. The shape of the beads irregular or not round makes the beads break easily. When the beads crack, the microbes can escape from immobilization matrix, rendering the process ineffective.[35]

3.2 Characterization of immobilization results

The results of characterizing immobilized UiO-66/GT beads in PVA-SA matrices using the SEM-EDX are shown in Fig. 2. The appearance of UiO-66/GT@PVA-SA beads (entire body) looks like fibers on the surface (Fig. 2a). The surface shape is probably the mycelium network of GT fungus. At a magnification of 5000 times, the surface texture of the beads appeared rough (Fig. 2b), whereas the surface of the beads coated with RB5 dye showed a relatively smooth texture (Fig. 2e).

From microscopic analysis of the beads' interior (Fig. 2c and f), it was revealed that the cavities were filled with a mixture of PVA and SA matrices. While MOF UiO-66 crystals could not be observed in the existing micrographs, their presence was confirmed by the results of EDX analysis. The results showed the presence of UiO-66 by the presence of the Zr element in the characterized beads. The histogram in Fig. 3 shows the elements contained in the beads before and after RB5 decolorization.

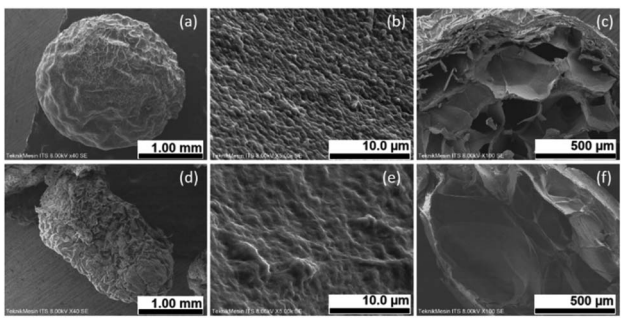

Fig. 2 SEM micrographs of UiO-66/GT@PVA-SA immobilized beads: (a) full body (40× magnification), (b) surface of the beads (5000× magnification), (c) cross-section (100× magnification); beads applied to RB5 dye: (d) full body (40× magnification), (e) surface of the beads (5000× magnification), (f) cross section (100× magnification).

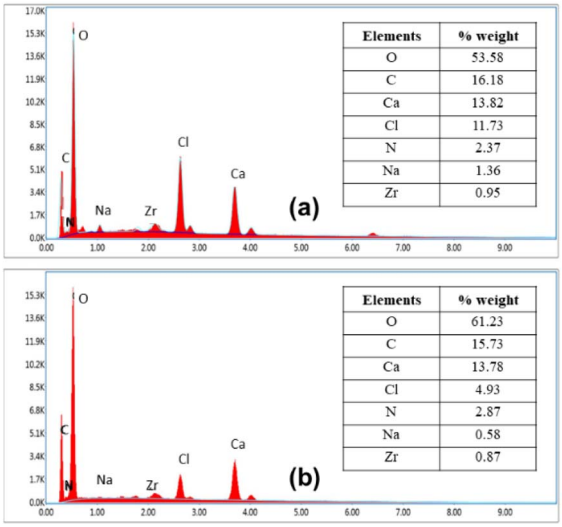

Elements	% weight
O	53.58
C	16.18
Ca	13.82
Cl	11.73
N	2.37
Na	1.36
Zr	0.95

Elements	% weight
O	61.23
C	15.73
Ca	13.78
Cl	4.93
N	2.87
Na	0.58
Zr	0.87

Fig. 3 Histogram of SEM-EDX: (a) UiO-66/GT@PVA-SA beads before decolorization and (b) UiO-66/GT@PVA-SA after decolorization.

The results from SEM-EDX analysis (Fig. 3) confirm that immobilized beads contain 0.95% zirconium (Zr) before decolorization and 0.87% after decolorization. The majority element in the beads is oxygen, indicating the presence of hydroxide and carboxylic groups from UiO-66, as well as hydroxides in PVA and SA. Interestingly, there was a reduction in Cl and Na elements after adsorption with RB5 dyes, which suggests the possibility of ion exchange/binding by sulfonate groups present in the chemical structure of RB5 or its metabolites. In addition, the binding of RB5 to the beads is proven by the addition of oxygen and nitrogen elements in the composite applied to RB5.

The characterization results of immobilized UiO-66 and GT fungus in PVA-SA composite using an X-ray diffractometer are

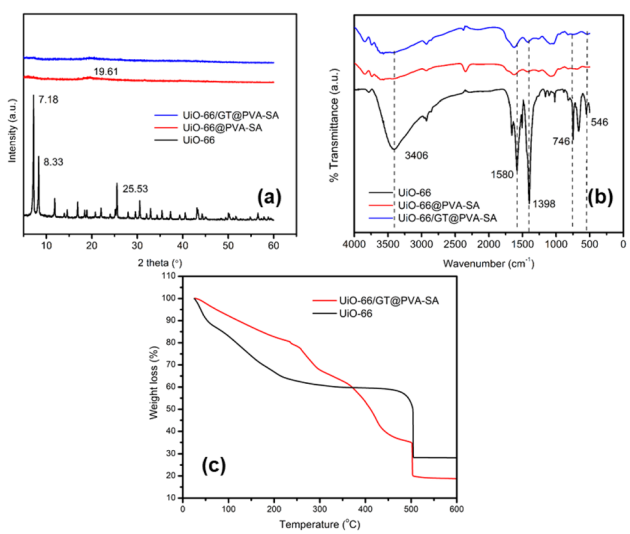

Fig. 4 (a) Diffractogram of UiO-66, UiO-66@PVA-SA, and UiO-66/GT@PVA-SA, (b) FTIR spectra of UiO-66 (black line), UiO-66@PVA-SA (red line), and UiO-66/GT@PVA-SA (blue line), and (c) the result of thermogravimetric analysis (TGA) of UiO-66 and UiO-66/GT@PVA-SA.

shown in Fig. 4a, showing the low intensity of the composite. Similarly, in the intensity shown in UiO-66 immobilized beads in PVA-SA matrices, the prominent intensity appears at an angle of 2 theta 19.61°, close to the specific diffraction peak of PVA, namely 2 theta = 20°.[36] On the other hand, pure UiO-66 gives high and medium intensity peaks at an angle of 2θ: 7.18, 8.33, and 25.53°. While after immobilization, the specific peaks of UiO-66 decreased, indicating that the crystallinity decreased. This reduction in crystallinity could be attributed to the destruction of UiO-66 crystals during the homogenization process or their coverage by the matrix and GT fungus mycelium.

The characterization of UiO-66 and immobilized beads with the FTIR spectrophotometer produced a spectrum, as shown in Fig. 4b. The beads UiO-66@PVA-SA and UiO-66/GT@PVA-SA display characteristic peaks similar to those of UiO-66, but the sharp peaks on UiO-66 experienced shifts and decreased in intensity when immobilized in PVA-SA matrices. The O–H vibration at 3406 cm^{-1} of the carboxylic group in UiO-66 molecule becomes a broad peak in immobilized composite. Similarly, UiO-66 peaks of 1580 and 1398 cm^{-1} are the C=O and C–O stretching of the carboxylate group. The Zr–O bending mode and Zr–(OC) stretching at 746 and 546 cm^{-1} almost disappear after becoming a composite.[37,38]

Fig. 4c displays the TGA results, revealing that both materials decompose at 500 °C. TGA analysis of UiO-66/GT@PVA-SA beads indicated a three-step process, involving the removal of water molecules, depolymerization of PVA-SA matrices, and pyrolysis and decomposition of organic ligands from UiO-66. During UiO-66 analysis, the thermal decomposition stage occurs in two stages: the first from 25–110 °C reduces water molecules by 38.1199%, followed by degradation of UiO-66 in the second stage at 110–500 °C.[39] While a slightly different TGA of UiO-66 was reported by Yang *et al.*, who stated that there were two successive stages, the first at a temperature of 25–400 °C corresponding to the removal of solvent molecules (including H_2O and DMF) and the second stage occurred at 400–800 °C causing damage to the molecular framework (framework) and appearance of metal oxide (ZrO_2).[40]

3.3 Decolorization of RB5 by UiO-66/GT@PVA-SA

To assess the ability of immobilized beads to decolorization RB5 dye, the combination of UiO-66 with live and dead (autoclaved) GT fungus was examined, and immobilized UiO-66 in PVA-SA matrices and immobilized GT fungus in the same matrices were used for comparison. Decolorization ability of UiO-66/GT(live)@PVA-SA beads was found to be 80.12%, indicating a significant percentage of RB5 removal as shown in Table 2. The highest decolorization rate by immobilized beads was achieved from the combination of UiO-66 with dead GT culture, which was 86.03% after an incubation period of 7 days.

In comparison, GT@PVA-SA and UiO-66@PVA-SA beads only achieved 53.98% and 33.25% decolorization. According to Alkas *et al.*, UiO-66 exhibited a decolorization efficiency of 99.29% for RB5 dye (100 mg L^{-1}) after 48 h, while UiO-66@GT composite achieved a decolorization efficiency of 72.55% after five days of incubation.[33] However, adsorption capacity of UiO-66 (133.333 mg g^{-1}) decreased significantly due to the obstruction of the active site by fungus mycelium and matrix, resulting in a maximum adsorption capacity of only 0.491 mg g^{-1} for RB5.

Immobilization of dead GT culture results in beads with a higher decolorization percentage. According to Fu and Viraraghavan, the use of dead cells as a biosorbent has advantages, including increased surface area due to cell rupture, easy procedure, and simple regeneration.[50] On the other hand, the evaluation of the reusability of the composite in decolorizing RB5 showed unsatisfactory results. Three cycles were carried out, resulting in 80%, 51%, and 21% decolorization percentages, respectively.

Table 3 shows the difference in decolorization ability of single elements and combined elements. The decolorization ability of UiO-66 which has a positive framework charge[51] proved to be very prominent against anionic dyes such as MO and RB5. While for cationic dyes (MB) the value is less satisfactory. While immobilizing fungi or bacteria has varying abilities depending on the enzymes they have. The combination of UiO-66 and fungus and PVA-SA matrix has quite good decolorization ability, but the weakness is that the contact time is still quite long compared to bacteria.

3.4 Adsorption of RB5 by UiO-66/GT@PVA-SA

3.4.1 Determination of the mass of the beads. In this RB5 adsorption experiment, the effect of the mass number of beads was tested on the percentage of RB5 decolorization. The mass beads variations were 1, 3, 5, and 7 g during the incubation period of 1, 3, and 7 days. Decolorization process was carried out under static conditions in an incubator at 30 °C. The percentage of decolorization obtained was shown in Fig. 5a. Decolorization index value is the percentage of decolorization divided by the mass of the beads, which was used to determine the best efficiency from the variations. The mass variation of the 3 g beads had the best efficiency in terms of the highest index

Table 2 Percentages of RB5 decolorization by the various beads

Contact time (days)	% Decolorization			
	GT@ PVA-SA	UiO-66 @PVA-SA	UiO-66/GT(live)@ PVA-SA	UiO-66/GT(dead)@ PVA-SA
Day 1	32.66 ± 0.10	27.67 ± 5.64	48.75 ± 0.25	70.17 ± 0.26
Day 3	42.58 ± 0.31	32.86 ± 0.07	65.72 ± 0.28	79.29 ± 0.04
Day 5	48.13 ± 0.21	33.12 ± 0.70	76.66 ± 0.10	82.66 ± 0.26
Day 7	53.98 ± 0.07	33.25 ± 0.10	80.12 ± 0.35	86.03 ± 0.13

Table 3 Various adsorbent in dye decolorization experiment as a comparison

Adsorbent	Dye	Decolorization rate (%) (contact time)	Ref.
UiO-66	Methyl orange (MO) (100 mg L^{-1}) MB (100 mg L^{-1})	96 & 54 (60 m)	41
UiO-66	MB (50 mg L^{-1})	~50 (500 m)	42
UiO-66	RB5 (100 mg L^{-1})	99.29 (48 h)	33
GT fungus (GT: *Gloeophyllum trabeum*)	MB (100 mg L^{-1})	76 (14 d)	43
UiO-66@GT	RB5 (100 mg L^{-1})	72.55 (5 d)	33
UiO-66@GT	MB (98 mg L^{-1})	88.99 (3 d)	In press
Immobilized GT-SA (sodium alginate)	RB5 (100 mg L^{-1})	53.08 (7 d)	44
Immobilized *Funalia trogii* fungus – SA	Acid black 52 (AB52) (100 mg L^{-1})	93.8 (13 d)	45
Immobilized *Coprinus plicatilis* fungus – SA	Reactive orange 16 (RO16) (100 mg L^{-1})	100 (20 h)	46
Immobilized *Trametes versicolor* fungus – SA	Phenol red (PR) (125 mg L^{-1})	89 (144 h)	47
Immobilized *Brevibacillus laterosporus bacteria & Galactomyces geotrichum yeast* – PVA-SA (PVA: Polyvinyl alcohol)	Reactive red (RR) (50 mg L^{-1})	100 (24 h)	48
Immobilized *Bacillus subtilis* (bacteria)-SA-PVA-bentonite	MB (50 mg L^{-1})	85.67 (24 h)	49
Immobilized UiO-66/GT@PVA-SA	MB (50 mg L^{-1})	88.29 (3 d)	22
Immobilized UiO-66/GT@PVA-SA	RB5 (50 mg L^{-1})	80.12 (7 d)	This work

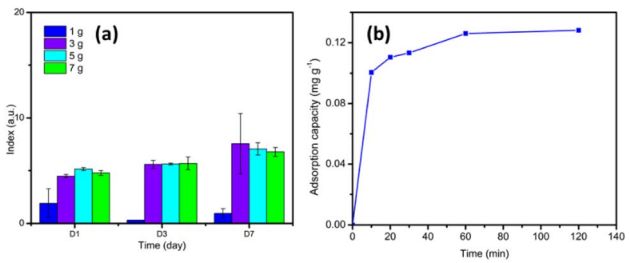

Fig. 5 (a) Decolorization index *versus* time, (b) effect of contact time.

value of 7.56. This number of beads was then used in subsequent tests such as isotherms, thermodynamics adsorption, and RSM optimization.

3.4.2 Effect of contact time. Based on adsorption test of the dye RB5 with the obtained biocomposite, it was found that adsorption of RB5 at a concentration of 50 mg L^{-1} using biocomposite UiO-66/GT@PVA-SA achieved an equilibrium time of 60 min as shown in Fig. 5b. Furthermore, there was an increase in adsorption capacity but tended to be relatively close, namely in the range of 0.12 mg g^{-1}. The equilibrium time is relatively fast compared to other studies using MOF UiO-66 as a dye adsorbent.

Other studies related to dye adsorption using UiO-66 as an adsorbent have been widely investigated, including Qiu *et al.* who reported the rapid absorption of pure UiO-66 to methyl orange (MO) dye concentration of 20 mg L^{-1} and adsorption was completed within 120 min with a capacity at the equilibrium of 70.4 mg g^{-1}.[52] While Mohammadi *et al.* reported adsorption equilibrium time of methylene blue (MB) with a concentration of 50 mg L^{-1} by UiO-66 after a time of 200 min and an adsorption capacity of 81 mg g^{-1}.[42] The unaffected adsorption capacity of UiO-66 in immobilized composite was probably due to the closure of the active sites of UiO-66 by GT mycelium and immobilized matrix.

3.4.3 Adsorption kinetics. The results of RB5 dye adsorption kinetics test using UiO-66/GT@PVA-SA biocomposite are shown in Table 4. These results confirm that RB5 adsorption process with immobilized beads follows a pseudo-second-order kinetic model. This is confirmed by the correlation coefficient (R^2) value, closer to 1 than the R^2 value of the pseudo-first-order kinetics. In addition, it is also proven from the value of the equilibrium adsorption capacity during the experiment ($Q_{e,\,exp}$) the value is closer to the value of q_e from the calculation results in the pseudo-second-order kinetics model of all temperature variations.

The confirmed pseudo-second-order adsorption kinetics model proves that adsorption process of adsorbate (RB5 dye) into the adsorbent is influenced by chemical bonds

Table 4 Kinetics parameters of pseudo-first- order and pseudo-second-order models

		Pseudo-first order			Pseudo-second order		
Temp	$Q_{e,\,exp}$	k_1	q_e	R^2	k_2	q_e	R^2
20 °C	0.077	0.025	0.139	0.137	17.059	0.076	0.999
30 °C	0.126	0.010	0.054	0.047	1.343	0.117	0.999
40 °C	0.096	0.002	0.056	0.004	2.884	0.086	0.987

(interactions) between the adsorbate and functional groups on the surface of the adsorbent.[53] Similarly, the kinetic model of Congo red adsorption by immobilized fungus in alginate and bentonite supporting matrix was also a pseudo-second-order model.[54] The pseudo-second-order kinetic model in adsorption of Congo red has an R^2 value close to one, and its adsorption capacity values (experimental Q_e and calculated q_e) are closer to the calculations of this model.

3.4.4 Isotherm adsorption studies. Adsorption mechanism between the adsorbent and the dye can also be explained by conducting isotherm adsorption experiments (adsorption at constant temperature), and the data obtained were then interpolated into the isotherm model (Langmuir and Freundlich). Furthermore, the Freundlich model is the isotherm adsorption model suitable for adsorption of RB5 by UiO-66/GT@PVA-SA, and it was observed from the correlation coefficient (R^2) value, which is higher than the Langmuir model. The results of interpolation in the isotherm adsorption model at 30 °C obtained the R^2 values of the Freundlich and Langmuir models, respectively 0.9348 and 0.8171. The graphs of the two models are shown in Fig. 6.

The Freundlich isotherm adsorption model showed that adsorption occurs on various/heterogeneous surfaces where the number of available surfaces is not the same and has different adsorption energies (multilayer).[5,55] Immobilization of GT fungus in alginate also led to the same result in previous studies and adsorption of the same dye (RB5) followed the Freundlich model.[44] This was also strengthened by the SEM micrograph showing the layers and cavities present in UiO-66/GT@PVA-SA beads (Fig. 2c), which have the potential to be active sites.

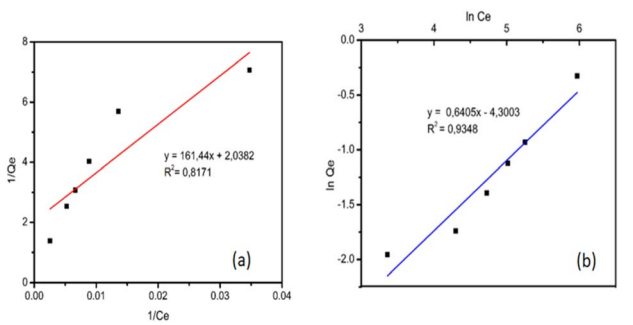

Fig. 6 Isoterm adsorption curves (a) Langmuir model and (b) Freundlich model.

The maximum adsorption capacity of biocomposite for RB5 dye in this study was found to be 0.491 mg g^{-1}, which is lower than the beads immobilized by GT fungus in alginate (0.5374 mg g^{-1}) as reported by Alkas *et al.*[44] Adsorption capacity value is much lower than the pure UiO-66, which has a maximum adsorption capacity of RB5 reaching 133.333 mg g^{-1}.[33]

3.4.5 Adsorption thermodynamics. To determine whether the dye adsorption process occurs spontaneously or not, it is important to consider the thermodynamic aspect of adsorption. The change in Gibbs free energy (ΔG^0) is an essential indicator for determining the spontaneity of a chemical reaction.[30] Other important thermodynamic parameters to obtain ΔG values are enthalpy (ΔH) and entropy (ΔS). In this RB5 adsorption study, the data for these parameters were obtained, as shown in Table 5.

The results of adsorption tests at temperature variations of 20, 30, and 40 °C found that the adsorbents investigated (UiO-66 and UiO-66/GT@PVA-SA) yielded negative ΔG values. The negative value of ΔG confirms that the adsorption process in nature is spontaneous and feasible.[56] In addition, there is a phenomenon from the two materials, when the system temperature is higher, the ΔG value also decreases. According to Saha and Chowdhury, a decrease in the negative value of ΔG^0 with increasing temperature indicates that adsorption process is more favorable at higher temperatures.[30] This is possible because the mobility of the adsorbate ions/molecules in solution increases with increasing temperature, and the affinity of the adsorbate for the adsorbent is higher at high temperatures.

The two adsorbents also show that adsorption process is exothermic regarding the negative ΔH value. According to Batouti *et al.*, the process is physisorption if the ΔH value is −4 to −40 kJ mol^{-1} and classified as chemisorption if −40 to −800 kJ.[57] Based on this classification, adsorption properties of UiO-66 and UiO-66/GT@PVA-SA tend to follow the type of physisorption. While the positive value of entropy (ΔS) indicates the degree of disorder of the adsorbate at the solid–liquid interface has increased during adsorption process. And the structural changes of the active site of the adsorbent are caused by increasing temperature.[58,59] The adsorbed solvent molecules are replaced by the adsorbate species, yielding more entropy shifts that allow randomness to occur in the system.[30] In this case, the solvent around the adsorbent is replaced with RB5 molecules, hence, the level of disorder of the adsorbate in adsorption process increases.

Table 5 Thermodynamic parameters of RB5 adsorption by UiO-66 and UiO-66/GT@PVA-SA

Adsorbents	T (K)	ΔG (kJ mol^{-1})	ΔH (kJ mol^{-1})	ΔS (J mol^{-1} K^{-1})
UiO-66	293.15	−42.086	−23.058	64.908
	303.15	−42.735		
	313.15	−43.384		
UiO-66/GT@PVA-SA	293.15	−8.459	−5.495	10.109
	303.15	−8.560		
	313.15	−8.661		

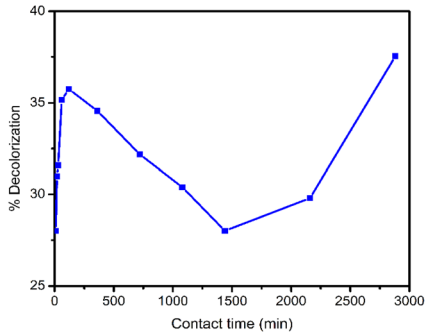

Fig. 7 RB5 decolorization rate at time variations.

3.5 RB5 decolorization mechanism

In decolorization process of RB5 dye with UiO-66 immobilized beads and GT fungus, the stages were estimated from the analysis results with UV-vis spectrophotometer and HPLC chromatography. The following shows a line curve of time against RB5 decolorization rate (Fig. 7) and a collection of HPLC chromatograms from RB5 control and treatment with time variations (Fig. 8).

Decolorization mechanism using biocomposite was proposed with the HPLC and UV-vis spectrophotometer. After obtaining the percentage of decolorization in various contact times (as shown in Fig. 7), it was found that decolorization rate decreased after 120 min (2 h) and increased again after 1440 min (24 h). RB5 dye adsorption process by biocomposite experienced saturation after reaching 120 min (2 h). Similarly, Ghorbani and Kamari stated that when saturated condition was achieved by the sorbent, all active sites were fulfilled and it could not adsorb much more dye molecules.[60] This phenomenon can happen for several reasons. First, after the active sites on the beads are filled with dye molecules, a repulsion phenomenon arises between the dye molecules bound to the beads and the dye molecules from the dye solution. This fact was also reported by Mohammadi *et al.*,[42] UiO-66 which has been saturated with MB dye, the adsorption value is reduced due to repulsion between the MB molecules. The second possibility is due to chemical bonds between the surfaces of the beads and the dye molecules are not too strong, hence, the dye molecules are released back into the solution.

According to Ashour *et al.*, as the contact time increases, the repulsive force between the dye molecules and the other molecules in the solution increases, making the opportunity to occupy the unfilled spots becomes more difficult. Their investigation found that adsorption of Crystal violet with the algae *Skeletonema costatum* also experienced the same after reaching the equilibrium time (120 min).[61] Due to this phenomenon, there was a decrease in the percentage of removal.

Chatterjee *et al.* showed that biological materials generally have a negative charge and can repel anionic dyes with strong electrostatic repulsion, resulting in poor dye adsorption.[62] In this case, PVA, SA, and GT fungus are considered organic materials, and RB5 dyes are also anionic dyes, so the possibility of repulsion is quite large. Due to this repulsion, the number of dye molecules in the solution increases again, and decolorization percentage decreases.

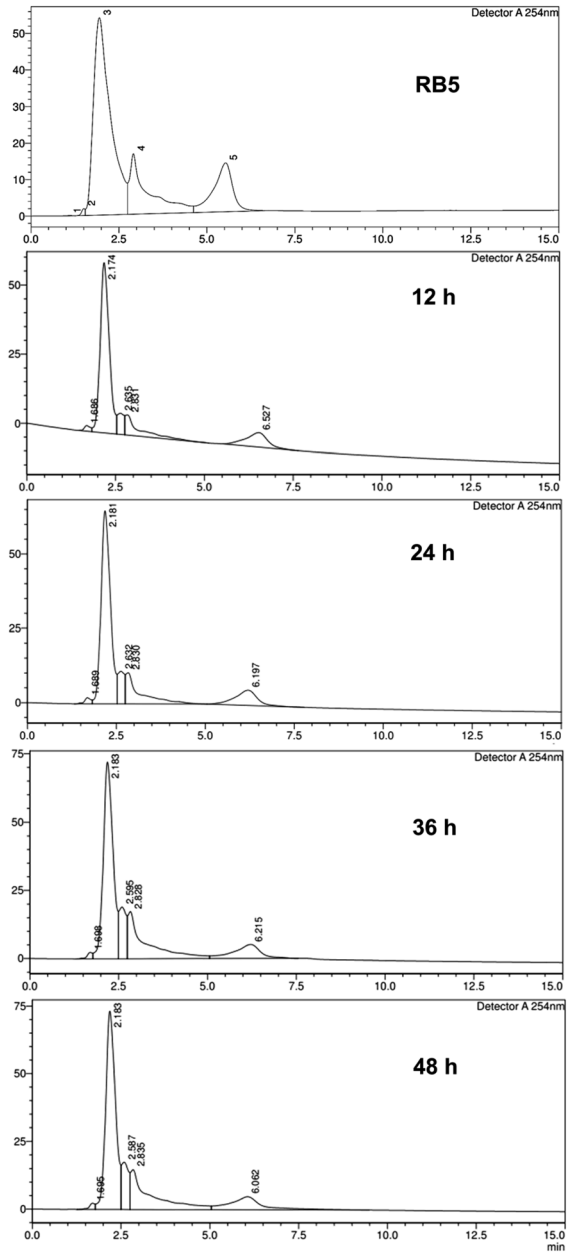

Fig. 8 A collection of HPLC chromatograms from RB5 control and treatment with time variations.

When the contact time reached 1440 min (24 h) (Fig. 7), there was an increase in decolorization percentage, indicating that the process was no longer solely an adsorption mechanism but also involved a degradation or biotransformation process reducing the number of RB5 molecules in the solution. The process of degradation or biotransformation in this system is due to the enzymatic action of GT fungus and the mechanism of the Fenton reaction, which produces hydroxyl radicals owned by GT fungus.[14,63,64] Therefore, decolorization mechanism involves an initial adsorption process, followed by degradation or biotransformation facilitated especially in the presence of GT fungus.

This observation confirms that the combination of GT and MOF UiO-66 differs from each substance's initial abilities. However, MOF UiO-66 can adsorb 99.29% RB5 dye in 48 h.[33] But when combined with GT fungus and PVA-SA matrices, this ability decreases due to the reduced surface area, and the active sites of UiO-66 are closed. Conversely, the pure GT fungus had a low decolorization ability of 36.47% after five days of contact,[33] which increased to 80.12% after immobilization with MOF UiO-66. This shows that decolorization ability of the composite against RB5 dye is quite good, increasing to about 43.65% of the pure GT fungus.

The chromatogram (Fig. 8) of the treatment compared to RB5 control focused at retention times of 2.909 min and 5.530 min. In the treatment with an incubation time of 12 h, there were different peaks, and a shift occurred. In this case, it proves that at the 12 h of incubation time, a process of degradation or biotransformation of RB5 dye has occurred. In the HPLC analysis method to detect dye degradation, this can be confirmed by a drastic shift of the main peak of the degraded dye[65] or the appearance of new peaks with varying retention times.[66] For comparison, Kumar *et al.*[67] reported that they obtained the degraded Rhodamine B (RhB) dye with the help of irradiation and the presence of Ag_2S–ZnS composite in Cellulose (AZCE). One peak of the RhB marker at a retention time of 7.35 min from the HPLC chromatogram of the control solution, when given this treatment, changed to shift to lower peaks at a retention time of 5.6–7 min. This indicates that degradation occurs which breaks down the RhB molecule into lower organic intermediate molecules.

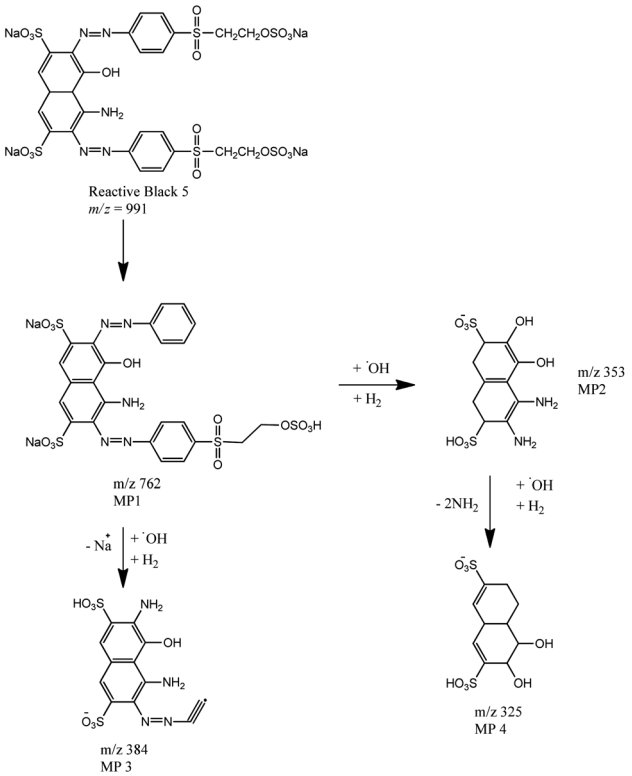

Fig. 9 Proposed RB5 Dye Degradation Pathway by UiO-66/GT@ PVA-SA biocomposite.

3.6 Identification of product metabolites and proposed RB5 degradation pathway

By comparing the chromatograms of RB5 dye and the samples with decolorization, four different peaks were identified as potential metabolites. These peaks were observed at each retention time: 1.21; 3.10; 3.77; and 16.80 min with the *m/z* value of each product metabolite 762.76 (MP 1); 353.02 (MP 2); 384.93 (MP 3); and 325.18 (MP 4), respectively.

Based on the identification of metabolite products, the proposed transformation or degradation pathway of RB5 by UiO-66/GT@PVA-SA biocomposite (Fig. 9) involves 3 mechanisms: desulphonation, oxidation, and deamination. Oxidation can occur with the help of hydroxyl radicals produced by GT brown-rot fungus through the Fenton reaction mechanism or from the production of extracellular enzymes such as laccase. The proposed pathway for the initial degradation of RB5 is hydrolysis which releases Na^+ ions and binds H^+ cations. Next, breaking the C–S bond attached to the benzene ring after the azo bond (–N=N–) forms the MP1 metabolite ($m/z = 762$). The MP1 species then reacts with the hydroxyl radical to form ion $m/z = 353$ (MP2), which is almost the same product found in the degradation of RB5 by UiO-66@GT composite ($m/z = 354$), originating from the Fenton reaction, asymmetric breaking, and hydrogenation.[33]

The formation of MP3 metabolite products ($m/z = 384$) may also involve enzymes or Fenton reaction with hydroxyl radicals. According to Legerská *et al.*, degradation of azo dyes with laccase enzymes begins with asymmetric termination of the azo bond (–N=N–) followed by termination of oxidation, desulphonation, deamination, demethylation, and dihydroxylation.[68] Similarly, in the formation of MP4 from MP2 metabolites, there are dehydroxylation and deamination reactions along with oxidation by hydroxyl radicals.

3.7 RB5 adsorption optimization using RSM

3.7.1 Statistical analysis. To determine the optimum conditions, the experiments were conducted using the Box-Behnken design, with the variations specified by Design Expert software version 13.0.5.0, which provided statistical analysis of the data collected. The data obtained were then analyzed using the software to find out the equation that represents the response to the three factors. Finally, the quadratic polynomial equation model was found to match the experimental data and this model was subsequently used to acquire the optimum conditions.

The quadratic polynomial equation model was selected and recommended by the software due to its high R^2 correlation coefficient of 0.9551 (95.51%). The results of the regression analysis confirmed that 95.51% of the variation in the equation model could be explained. Furthermore, ANOVA analysis was performed to verify the equation model, the results of the program analysis are listed in Table 5. The results analysis obtained a *p*-value of 0.0071, this shows that the quadratic equation model is significant. According to M-Ridha *et al.*, the

significance level of the model applied can be confirmed by the relatively high R^2 value. While the proper precision value of the model (adequate precision) which is greater than 4 indicates a comparison of the signal to noise.[69] In this study, the adequate precision value was obtained at 13.3680 indicating that the acquired signal was sufficient. Significant model indicators are also seen from the Lack of Fit F-value, which is not significant, further confirming the suitability of the equation model.

Table 6 also shows that the parameters of dye concentration and pH alone had a significant effect on decolorization response as indicated by a p-value < 0.05 (0.0014 and 0.0379). Although the temperature did not have a significant effect, all variables are important independent parameters that have been previously studied to influence the dye decolorization process.[32,60] The interaction between concentration and temperature parameters in this model was also shown to significantly affect the percent decolorization response of RB5 by UiO-66/GT@PVA-SA biocomposite. Other parameters that have a significant effect are the quadratic parameters of concentration and pH marked by a p-value < 0.05 (0.0340 and 0.0036).

The following equation is a polynomial model where Y is decolorization rate response and the equation was predicted from the software after processing all decolorization rates of each variation:

$$Y = 58.13 - 5.97X_1 + 2.63X_2 - 2.14X_3 - 0.2932X_1 \cdot X_2 + 3.75X_1 \cdot X_3 - 3.07X_2 \cdot X_3 + 3.99{X_1}^2 - 7.12{X_2}^2 + 1.65{X_3}^2 \quad (12)$$

In general, an overview of the effect can be seen from the p-value and the constants of each parameter. This can also be seen from the nature of the single-factor effect from the initial concentration of RB5 dye and temperature, which are negative, while the effect of pH is positive. The results of the Design Expert programming analysis with the eqn (12) model, obtained the optimum conditions for the three independent variables as follows: dye concentration at 50 mg L^{-1}, pH = 8.152, and temperature = 20 °C.

3.7.2 Interactions effect of two variables. The three-dimensional (3D) response surface graph is very helpful in showing a function of two factors where the other factors are set at a certain level, this is performed to test the interactions between factors and responses.[60] Fig. 10 illustrates the three-dimensional response surface of the effects of different parameters in RB5 decolorization process by UiO-66/GT@PVA-SA biocomposite.

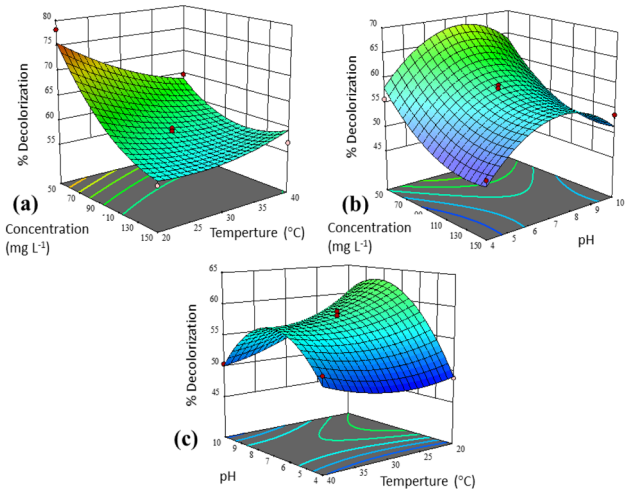

Fig. 10 3D response surface graphs for two different variables: (a) interaction of concentration and temperature, (b) interaction of concentration and pH, and (c) interaction of pH and temperature.

The interaction of concentration and temperature in decolorization process from Fig. 10a at constant pH (7) shows that the degree of decolorization increases at low temperatures (20 °C) and concentration (50 mg L^{-1}). Slightly different, UiO-66@GT biocomposite in the same interaction achieved the highest decolorization value at about 35 °C with the same concentration (50 mg L^{-1}).[33] While Daâssi *et al.* confirmed that at higher concentrations (above 200 mg L^{-1}), the decrease in decolorization of Lanaset Gray (LG) dye was reduced due to the inhibition of fungus growth and cell metabolic activity due to the toxic nature of the dye.[70] Yadav *et al.* also reported that there are significant interactions between independent parameters and dependent factors. There was an optimal decolorization by laccase at 35 °C, followed by a decrease and an asynchronous downward trend as the dye concentration increased.[71]

Table 6 ANOVA results from RSM analysis

Source	Sum of squares	df	Mean square	F-value	p-value	
Model	748.36	9	83.15	11.83	0.0071	Significant
X_1-concentration	285.37	1	285.37	40.60	0.0014	
X_2-pH	55.15	1	55.15	7.85	0.0379	
X_3-temperature	36.49	1	36.49	5.19	0.0717	
$X_1 \cdot X_2$	0.3439	1	0.3439	0.0489	0.8337	
$X_1 \cdot X_3$	56.21	1	56.21	8.00	0.0368	
$X_2 \cdot X_3$	37.64	1	37.64	5.36	0.0685	
${X_1}^2$	58.89	1	58.89	8.38	0.0340	
${X_2}^2$	187.40	1	187.40	26.66	0.0036	
${X_3}^2$	10.08	1	10.08	1.43	0.2847	
Residual	35.15	5	7.03			
Lack of fit	32.61	3	10.87	8.56	0.1064	Not significant
Pure error	2.54	2	1.27			
Cor total	783.50	14				

The interaction between concentration and pH factors (Fig. 10b) showed the highest decolorization value at a concentration of 50 mg L^{-1} and pH of about 7. On the other hand, the interaction of pH and temperature (Fig. 10c) produces a saddle graph, which shows the highest decolorization rate at 20° and a pH of about 7. According to Das and Mishra, substantial variations in pH and temperature values can affect the three-dimensional shape of enzymes in microorganisms as well as their usability.[32]

4 Conclusion

This study successfully synthesized and characterized a new composite UiO-66/GT@PVA-SA. The composite demonstrated superior degradation capabilities for the synthetic dye RB5 compared to pure GT culture. The percentage of RB5 decolorization with pure GT culture was only 36.47%, while UiO-66/GT@PVA-SA biocomposite achieved a decolorization rate of 80.12%. The potential for composite reusability was assessed for three cycles. Decolorization ability for immobilized UiO-66/GT was 21% in the 3rd cycle. In addition, the maximum adsorption capacity of UiO-66/GT@PVA-SA biocomposite against RB5 was determined to be 0.491 mg g^{-1}. Adsorption kinetics model followed a pseudo-second-order mechanism with an R^2 value of 0.9997 at 30 °C, and the suit isotherm adsorption model was found to be the Freundlich isotherm model. The thermodynamics analysis indicated that RB5 adsorption by biocomposite is spontaneous and feasible with a negative ΔG value. The metabolite products produced during decolorization process were identified, with four metabolites predicted as follows: $C_{24}H_{19}N_5Na_2O_{13}S_4$ (m/z = 762), $C_{10}H_{13}N_2O_8S_2^-$ (m/z = 353), $C_{12}H_9N_4O_7S_2^-$ (m/z = 384), and $C_{10}H_{13}O_8S_2^-$ (m/z = 325). While the results of RSM analysis revealed the optimal conditions for RB5 decolorization by composition for the following three independent variables: dye concentration at 50 mg L^{-1}, pH = 8.152, and temperature = 20 °C.

Author contributions

TRA: conceptualization, methodology, validation, formal analysis, investigation, writing – original draft, writing – review & editing, visualization. ASP: conceptualization, methodology, validation, resources, writing – original draft, writing – review & editing, supervision, funding acquisition. RE: writing – original draft, writing – review & editing, supervision. TE: writing – original draft, supervision.

Conflicts of interest

There are no conflicts to declare.

Acknowledgements

The authors express profound gratitude to the Indonesian Endowment Fund of Education/Lembaga Pengelola Dana Pendidikan (LPDP) for their financial support and the Samarinda State Agricultural Polytechnic Director for giving a chance to continue the doctoral program.

References

1 A. B. Ayed, B. Hadrich, G. Sciara, A. Lomascolo, E. Bertrand, C. B. Faulds, H. Zouari-Mechichi, E. Record and T. Mechichi, *Microorganisms*, 2022, **10**, 1137.
2 G. C. de Oliveira Neto, J. M. Ferreira Correia, P. C. Silva, A. G. de Oliveira Sanches and W. C. Lucato, *J. Cleaner Prod.*, 2019, **228**, 1514–1525.
3 B. Huang, J. Zhao, Y. Geng, Y. Tian and P. Jiang, *Resour., Conserv. Recycl.*, 2017, **119**, 69–77.
4 A. Hasanbeigi and L. Price, *Renewable Sustainable Energy Rev.*, 2012, **16**, 3648–3665.
5 M. T. Yagub, T. K. Sen, S. Afroze and H. M. Ang, *Adv. Colloid Interface Sci.*, 2014, **209**, 172–184.
6 B. Lellis, C. Z. Fávaro-Polonio, J. A. Pamphile and J. C. Polonio, *Biotechnol. Res. Innov.*, 2019, **3**, 275–290.
7 W. Zhou, X. Chen, M. Ismail, L. Wei and B. Hu, *Chemosphere*, 2021, **275**, 130025.
8 A. S. Purnomo, in *Microbe-Induced Degradation of Pesticides*, ed. S. N. Singh, Springer International Publishing, Cham, 2017, pp. 1–22.
9 B. Nabilah, A. S. Purnomo, D. Prasetyoko and A. A. Rohmah, *Arabian J. Chem.*, 2023, **16**, 104940.
10 N. Aliasgharlou, M. Bahram, P. Zolfaghari and N. Mohseni, *Turk. J. Chem.*, 2020, **44**, 987–1001.
11 E. S. Hartikainen, O. Miettinen, A. Hatakka and M. A. Kähkönen, *Am. J. Environ. Sci.*, 2016, **12**, 77–85.
12 R. T. Mahmood, Biodegradation of textile dyes by indigenously isolated brown rot fungi and study of their enzyme system, PhD thesis, Arid Agriculture University, 2017.
13 N. Park and S.-S. Park, *Int. J. Biol. Macromol.*, 2014, **70**, 583–589.
14 A. S. Purnomo, V. T. Mauliddawati, M. Khoirudin, A. F. Yonda, R. Nawfa and S. R. Putra, *Int. J. Environ. Sci. Technol.*, 2019, **16**, 7555–7564.
15 H. D. Rizqi and A. S. Purnomo, *World J. Microbiol. Biotechnol.*, 2017, **33**, 92.
16 J. Ha, C. R. Engler and J. R. Wild, *Bioresour. Technol.*, 2009, **100**, 1138–1142.
17 S. Rodríguez Couto, *Biotechnol. Adv.*, 2009, **27**, 227–235.
18 H. Liu, L. Guo, S. Liao and G. Wang, *J. Appl. Microbiol.*, 2012, **112**, 651–659.
19 T. Hu, Q. Liu, T. Gao, K. Dong, G. Wei and J. Yao, *ACS Omega*, 2018, **3**, 7523–7531.
20 S. E. Moradi, S. Dadfarnia, A. M. Haji Shabani and S. Emami, *Turk. J. Chem.*, 2017, **41**, 426–439.
21 R. Ediati, L. L. Zulfa, K. A. Nugroho, A. Mukminin, D. O. Sulistiono, M. Nadjib and Y. Kusumawati, *IOP Conf. Ser.: Mater. Sci. Eng.*, 2019, **578**, 012072.
22 T. R. Alkas, A. S. Purnomo, A. N. Pratiwi, Y. Nurwijayanti, R. Ediati, T. Ersam and Y. Kusumawati, *Mater. Today Chem.*, 2023, **29**, 101411.

23 A. S. Purnomo, A. S. Prameswari, H. D. Rizqi, T. R. Alkas, R. Ediati and Y. Kusumawati, *Int. J. Technol.*, 2022, **13**, 1768.
24 H. Tehubijuluw, R. Subagyo, M. F. Yulita, R. E. Nugraha, Y. Kusumawati, H. Bahruji, A. A. Jalil, H. Hartati and D. Prasetyoko, *Environ. Sci. Pollut. Res.*, 2021, **28**, 37354–37370.
25 S. Lagergren, *K. Sven. Vetenskapsakad. Handl.*, 1898, **24**, 1–39.
26 Y. S. Ho and G. McKay, *Process Biochem.*, 1999, **34**, 451–465.
27 I. I. Laskar and Z. Hashisho, *Sep. Purif. Technol.*, 2020, **241**, 116681.
28 N. Yuan, H. Cai, T. Liu, Q. Huang and X. Zhang, *Adsorpt. Sci. Technol.*, 2019, **37**, 333–348.
29 M. Benjelloun, Y. Miyah, G. Akdemir Evrendilek, F. Zerrouq and S. Lairini, *Arabian J. Chem.*, 2021, **14**, 103031.
30 P. Saha and S. Chowdhury, in *Thermodynamics*, InTech, 2011, pp. 349–364.
31 S. P. Varghese, A. T. Babu, B. Babu and R. Antony, *J. Water Process. Eng.*, 2017, **19**, 1–7.
32 A. Das and S. Mishra, *J. Environ. Chem. Eng.*, 2017, **5**, 612–627.
33 T. R. Alkas, R. Ediati, T. Ersam, R. Nawfa and A. S. Purnomo, *Arabian J. Chem.*, 2022, **15**, 104129.
34 M. S. Usha, B. Sasirekha, R. B. Bela, S. Devi, C. Kamalini, G. A. Manasa and P. M. Neha, *J. Sci. Ind. Res.*, 2012, **71**, 504–510.
35 B.-B. Lee, P. Ravindra and E.-S. Chan, *Chem. Eng. Technol.*, 2013, **36**, 1627–1642.
36 V. V. Phatake, A. A. Mishra and B. M. Bhanage, *Inorganica Chim. Acta*, 2020, **501**, 119274.
37 M. A. R. Pambudi, N. Prayogo, M. Nadjib and R. Ediati, *Indones. J. Chem. Res.*, 2021, **8**, 183–193.
38 Z. Jin and H. Yang, *Nanoscale Res. Lett.*, 2017, **12**, 539.
39 M. Athar, P. Rzepka, D. Thoeny, M. Ranocchiari and J. Anton van Bokhoven, *RSC Adv.*, 2021, **11**, 38849–38855.
40 Z. Yang, J. Cao, Y. Chen, X. Li, W. Xiong, Y. Zhou, C. Zhou, R. Xu and Y. Zhang, *Microporous Mesoporous Mater.*, 2019, **277**, 277–285.
41 A. R. Putra Hidayat, L. L. Zulfa, A. R. Widyanto, R. Abdullah, Y. Kusumawati and R. Ediati, *RSC Adv.*, 2023, **13**, 12320–12343.
42 A. A. Mohammadi, A. Alinejad, B. Kamarehie, S. Javan, A. Ghaderpoury, M. Ahmadpour and M. Ghaderpoori, *Int. J. Environ. Sci. Technol.*, 2017, **14**, 1959–1968.
43 A. S. Purnomo, N. A. Ubaidillah, H. D. Rizqi, R. Nawfa and H. S. Putro, *ASM Sci. J.*, 2021, **16**, 100–106.
44 T. R. Alkas, R. Ediati, T. Ersam and A. S. Purnomo, *Mater. Today: Proc.*, 2022, S2214785322011804.
45 C. Park, B. Lee, E.-J. Han, J. Lee and S. Kim, *Enzyme Microb. Technol.*, 2006, **39**, 371–374.
46 H. A. Akdogan and M. Canpolat, *Fibers Polym.*, 2013, **14**, 76–81.
47 A. Krastanov, R. Koleva, Z. Alexieva and I. Stoilova, *Biotechnol. Biotechnol. Equip.*, 2013, **27**, 4263–4268.
48 M. B. Kurade, T. R. Waghmode, J.-Q. Xiong, S. P. Govindwar and B.-H. Jeon, *J. Cleaner Prod.*, 2019, **213**, 884–891.
49 A. A. Rohmah, A. S. Purnomo and W. N. Safitri, *Indones. J. Chem.*, 2022, **22**, 1637.
50 Y. Fu and T. Viraraghavan, *Bioresour. Technol.*, 2001, **79**, 251–262.
51 X. Li, H. Zhang, P. Wang, J. Hou, J. Lu, C. D. Easton, X. Zhang, M. R. Hill, A. W. Thornton, J. Z. Liu, B. D. Freeman, A. J. Hill, L. Jiang and H. Wang, *Nat. Commun.*, 2019, **10**, 2490.
52 J. Qiu, Y. Feng, X. Zhang, M. Jia and J. Yao, *J. Colloid Interface Sci.*, 2017, **499**, 151–158.
53 A. N. Ebelegi, N. Ayawei and D. Wankasi, *Open J. Phys. Chem.*, 2020, **10**, 166–182.
54 M. T. M. H. Hamad and M. S. S. Saied, *Appl. Water Sci.*, 2021, **11**, 35.
55 A. Oussalah, A. Boukerroui, A. Aichour and B. Djellouli, *Int. J. Biol. Macromol.*, 2019, **124**, 854–862.
56 E. Gunasundari, P. Senthil Kumar, N. Rajamohan and P. Vellaichamy, *Desalin. Water Treat.*, 2020, **192**, 358–370.
57 M. E. Batouti, W. Sadik, A. G. Eldemerdash, E. Hanafy and H. A. Fetouh, *Polym. Bull.*, 2023, **80**, 4965–4989.
58 T. Tian, Y. Jia, J. Wu, J. Zhao, K. Xu, Z. Wang and Z. Wang, *Desalin. Water Treat.*, 2021, **244**, 226–240.
59 Asranudin, Holilah, A. S. Purnomo, H. Bahruji, D. Allouss, I. El Alaoui-Elbalrhiti, R. Subagyo, A. A. Rohmah and D. Prasetyoko, *RSC Adv.*, 2023, **13**, 790–801.
60 F. Ghorbani and S. Kamari, *Adsorpt. Sci. Technol.*, 2017, **35**, 317–338.
61 M. Ashour, A. E. Alprol, M. Khedawy, K. M. Abualnaja and A. T. Mansour, *Materials*, 2022, **15**, 6375.
62 S. Chatterjee, S. Chatterjee, B. P. Chatterjee and A. K. Guha, *Colloids Surf., A*, 2007, **299**, 146–152.
63 N. I. Pratiwi, A. S. Purnomo, H. D. Rizqi, T. R. Alkas and R. Nawfa, *AIP Conf. Proc.*, 2021, **2349**, 020076.
64 A. S. Purnomo, N. E. A. Andyani, R. Nawfa and S. R. Putra, *AIP Conf. Proc.*, 2020, **2237**, 020002.
65 S. Thangaraj, B. Jooju and S. Kumar Sadasivam, *Appl. Ecol. Environ. Sci.*, 2021, **9**, 203–208.
66 U. Tahir and A. Yasmin, *Braz. J. Microbiol.*, 2021, **52**, 761–771.
67 T. K. M. P. Kumar and S. K. A. Kumar, *Photochem. Photobiol. Sci.*, 2019, **18**, 148–154.
68 B. Legerská, D. Chmelová and M. Ondrejovič, *Nova Biotechnol. Chim.*, 2016, **15**, 90–106.
69 M. J. M-Ridha, S. I. Hussein, Z. T. Alismaeel, M. A. Atiya and G. M. Aziz, *Alexandria Eng. J.*, 2020, **59**, 3551–3563.
70 D. Daâssi, T. Mechichi, M. Nasri and S. Rodriguez-Couto, *J. Environ. Manage.*, 2013, **129**, 324–332.
71 A. Yadav, P. Yadav, A. K. Singh, V. Kumar, V. C. Sonawane, Markandeya, R. N. Bharagava and A. Raj, *Bioresour. Technol.*, 2021, **340**, 125591.